Lipopolysaccharide promotes the osteoclastogenesis through the autophagic degradation of TNF receptor-associated factor 3

Jing Hu[a], **Xianyou Zeng**[a], **Chengcheng Song**[b,*], **Lei Zhang**[b,*]

[a] Department of Stomatology, The Affiliated Hospital of Jinggangshan University, Ji'an, Jiangxi 343000 China
[b] Department of Stomatology, Dujiangyan people's Hospital, Chengdu, Sichuang 611800 China

*Corresponding authors, e-mail: SCCDJY@yeah.net, 282772709@qq.com

ABSTRACT: Lipopolysaccharide (LPS) is a pro-osteoclastogenic factor and autophagic activator. TNF receptor-associated factor (TRAF) 3, an anti-osteoclastogenic factor, can be degraded by autophagic activation. The effect of LPS on the level of TRAF3 during the osteoclastogenesis keeps vague. In this study, we investigated the roles of LPS in the expression patterns of TRAF3 *in vivo* and *in vitro*. Combined with the application of autophagic pharmacological inhibitors, we observed the significance of LPS-regulated autophagy in TRAF3 protein level. Moreover, we explored the effects of TRAF3 on LPS-induced osteoclastogenesis using gain-of-function and loss-of-function assays *in vitro*. Our study showed that LPS could reduce the protein level of TRAF3 in osteoclast precursors (OCPs) *in vitro* and *in vivo*, while no affecting the mRNA expression of TRAF3. In addition, TRAF3 overexpression reversed LPS-induced osteoclastogenesis. Importantly, LPS-inhibited TRAF3 protein level was recovered by autophagic inhibition with chloroquine or bafilomycin. Furthermore, LPS-induced osteoclastogenesis was suppressed by chloroquine, which was reversed by TRAF3 silencing. In conclusion, LPS can promote the autophagic degradation of TRAF3, which serves as an indispensable underlying mechanism in LPS-induced osteoclastogenesis.

KEYWORDS: LPS, osteoclastogenesis, autophagy, TRAF3, osteoclast precursors

INTRODUCTION

Osteoclasts and osteoblasts are functional cells that mediate bone resorption and bone formation, respectively, which maintains bone homeostasis [1]. In chronic infections caused by Gram-negative bacteria such as periodontitis and osteomyelitis, the number and activity of osteoclasts increase, which destroys bone homeostasis and results in osteoporosis [2]. At present, the main treatment of these diseases is limited to dental/surgical repair, antibiotics, and non-surgical mechanical debridement [3]. Lipopolysaccharide (LPS) is a main component of the outer membrane of Gram-negative bacteria, which can cause inflammation [4, 5]. *In vivo* assays showed that LPS promotes the osteoclastic activity by upregulating the expression of Receptor Activator for Nuclear Factor-κB Ligand (RANKL) [6]. However, LPS can directly promote the osteoclastogenesis independent of RANKL in osteoclast precursors, and RANKL antibody treatment cannot block LPS-induced osteoclastogenesis [7, 8]. At present, the mechanism regarding LPS-induced osteoclastogenesis *in vitro* has been well reported. Under LPS intervention, TLR4 (the receptor of LPS) expression increases with osteoclast formation and survival. In addition, the enhancement of TRAF6 gene expression also exists in LPS-induced osteoclast differentiation [9, 10]. In the early stage of LPS-induced osteoclastogenesis, the expressions of NF-κB, p-P-38, p-JNK, and p-ERK are all upregulated [11, 12]. Furthermore, under LPS intervention, the crucial osteoclastogenic factor, nuclear factor of activated T cells

c1 (NFATc1), increases in the nucleus, subsequently inducing the mRNA expression of osteoclastic markers including tartrate-resistant acid phosphatase (TRAP), MMP-9, Atp6v0d2, cathepsin K, and β3-integrin [12]. However, there are still many issues to be clarified in LPS-induced osteoclastogenesis.

Autophagy is a highly conserved intracellular metabolic process, which maintains intracellular homeostasis. Autophagy has been proved to be involved in the proliferation and differentiation of osteoclasts. As an important cascade downstream of JNK1, a novel autophagy pathway participates in RANKL-induced osteoclastogenesis [13]. In addition, although estrogen and curcumin have anti-osteoclastic function, they can activate autophagy, whereby playing a negative effect on the above effects [14, 15]. Therefore, suppressing autophagy can enhance the anti-osteoclastic effect of estrogen or curcumin [14, 15]. Similar results have been reported in other investigations [16–18]. As a member of TRAF family, TRAF3-connected NF-κB-inducing kinase (NIK) can be structurally degraded by the ubiquitination mediated by cellular inhibitor of apoptosis (cIAP) [19], subsequently inhibiting NF-κB activity [20, 21]. Thus, TRAF3 is essential to the inhibition of cell proliferation and survival. Xiu et al [22] proved that TRAF3 is an inhibitor of osteoclastogenesis. Furthermore, autophagy plays an essential role in RANKL-mediated TRAF3 degradation, thus promoting the osteoclastogenesis. The related studies also confirmed that autophagy enhances the osteoclastogenesis through TRAF3 degradation [23, 24]. Overall, the autophagic degradation

of TRAF3 is a key factor of osteoclastogenesis.

LPS is widely considered an autophagic activator. LPS can mediate the activation of hepatic stellate cells by inducing autophagy [25]. LPS can downregulate the osteogenic/odontogenic differentiation of apical papilla stem cells by inducing autophagy [26]. LPS induces autophagy in human nasal epithelial cells through targeting the AMPK-mTOR pathway [27]. More importantly, LPS-induced autophagy is an important factor for the enhanced osteoclastogenesis, which has been reported in several studies. However, the underlying mechanism regarding LPS-regulated autophagy during the osteoclastogenesis remains unclear. We hypothesized that LPS may promote the degradation of TRAF3 by activating autophagy, thus inducing the osteoclastogenesis. To test this hypothesis, we examined the effects of LPS on the expression patterns of TRAF3 *in vivo* and *in vitro*. Combined with autophagic pharmacological inhibitors, we observed the role of LPS-regulated autophagy in TRAF3 protein level. Furthermore, we explored the roles of TRAF3 in LPS-induced osteoclastogenesis using gene overexpression or silencing techniques *in vitro*.

MATERIALS AND METHODS

Reagents

LPS, chloroquine, bafilomycin A1, and TRAP staining kit were obtained from Sigma-Aldrich (St. Louis, USA). After dissolved in 1% BSA, different working concentrations of LPS were prepared by complete α-Minimum Eagle's Medium (α-MEM).

Isolation and induction of OCPs

Six-week-old littermate C57BL/6J female mice were purchased from GemPharmatech Co., Ltd (Nanjing, China). The mice were killed after cervical dislocation, and the tibiae were flushed with α-MEM without serum. Bone marrow cells were incubated with α-MEM containing 10% FBS, penicillin (100 U/ml), and streptomycin (100 mg/ml) for 24 h. After the treatment with M-CSF (20 ng/ml) for 3 days, non-adherent cells were collected, and adherent cells (Bone Marrow-derived macrophages; BMMs) were used as OCPs. The cells were cultured at 37 °C in moist air containing 5% CO_2.

Osteoclast formation assay

OCPs (2×10^4/well) were incubated in a 48-well plate in α-MEM containing LPS (100 ng/ml) for 4 days to form osteoclasts. Osteoclast formation was detected by TRAP staining using Leukocyte Acid Phosphatase Kit (Sigma-Aldrich). TRAP$^+$ cells with more than 3 nuclei were considered the osteoclasts.

Lentiviral transduction

Lentiviruses encoding TRAF3 (including corresponding control vector) were constructed by homologous recombination between expression vector (EX-Puro-Lv105) and cDNA in 293 cells using the construction kit (GeneCopoeia, Maryland, USA) according to manufacturer's protocols. After 2 days, the supernatants were harvested, and OCPs were incubated in the virus solution containing 8 μg/ml polybrene at MOI 10 lasted for 2 days. Puromycin (7.5 μg/ml) was used to screen the infected cells. The overexpression efficiency of viral genes was evaluated by Western-blot assays.

siRNA transfection

Control siRNAs and siRNAs against mouse TRAF3 were obtained from Thermo Fisher Scientific (Massachusetts, USA). The target sequences were as follows: Control, 5′-GCAAGCGTCACTCGGTTTA-3′; TRAF3, 5′-GCAGTGAGCCTCACTGTTA-3′. The indicated cells were cultured in 6-well plates and then transfected with siRNAs (100 pmol/well) using RNAiMAX (Thermo Fisher Scientific) in accordance with manufacturer's protocols. For 48 h, the silence efficiency of siRNAs was assessed by Western-blot experiments.

Western-blotting

The lysates of the indicated cells were prepared, separated on 10% SDS-PAGE gels, and transferred to polyvinylidene fluoride membranes (PVDF, Thermo Fisher Scientific), which were incubated with the specific antibodies against TRAF3 (4729), LC3 (3868), p62 (23214), and GAPDH (Cell Signaling Technology, Massachusetts, USA). Horseradish peroxidase (HRP)-linked secondary antibodies were applied to visualize the immunoreactivity under a chemiluminescence system (Omega Lum G, Aplegen, California, USA).

Quantitative real-time PCR (qRT-PCR) analysis

The total RNA was extracted and purified by the TRIzol method. Synthesis of cDNA and qRT-PCR measurements were carried out in accordance with manufacturer's protocols. The pre-designed primer sequences for qPCR were as follows:

Matrix metalloproteinase-9 (MMP-9), 5′-CAAAGA CCTGAAAACCTCCAAC-3′ (sense) and 5′-GACTGCTT CTCTCCCATCATC-3′ (anti-sense);

TRAP, 5′-GCTGGAAACCATGATCACCT-3′ (sense) and 5′-TTGAGCCAGGACAGCTGAGT-3′ (anti-sense);

Cathepsin K (CTSK), 5′-GGAAGAAGACTCACCAG AAGC-3′ (sense) and 5′-GTCATATAGCCGCCTCCACA G-3′ (anti-sense);

TRAF3, 5′-CCAAGAAAGCATCATCAAACAC-3′ (sense) and 5′-TCATTCGGACAGTAGACCTGAA-3′ (anti-sense);

GAPDH, 5′-GGTGAAGGTCGGTGTGAACG-3′ (sense) and 5′-CTCGCTCCTGGAAGATGGTG-3′ (anti-sense).

Relative expression was calculated using the $2^{-\Delta\Delta Ct}$ method.

GAPDH was used as the internal reference. qRT-PCR was carried out using SYBR Premix Ex Taq™ kit (TakaRa, Tokyo, Japan) and ABI7500 PCR system (Applied Biosystems, Thermo Fisher Scientific) in accordance with manufacturer's protocols.

Animal experiments

Sixteen 6-week-old C57/BL6 male mice (20 ± 2.5 g) were purchased from the Animal Center of GemPharmatech Co., Ltd (Nanjing, China). The mice were housed in a common environment in which the room temperature was 20–30 °C and the humidity was 60–80% and received a general laboratory diet (Agway RMH 3000 animal chow: Arlington Heights, Illinois, USA). All mice were randomly divided into control group (PBS-treated) and experimental group (LPS-treated) ($n = 8$/group). On both day 1 and day 5, intraperitoneal PBS or LPS (5 mg/kg weight) injections were performed. After 9 days, the mice were anesthetized with isoflurane (2%, Inhalation anaesthesia) and sacrificed via cervical dislocation, and their femurs were collected and fixed in 4% paraformaldehyde (PFA). Blood samples were centrifuged for serum isolation and stored in −80 °C for ELISA analysis. Before sacrificed, Bone Mineral Density (BMD) was determined by Dual energy X-ray absorptiometry (DXA, PIX-Imus2; Lunar, Wisconsin, USA). The mice were anesthetized with pentobarbital sodium and fixed on the test bed in prone position. BMD was measured through whole body scanning, and the parameters were automatically provided by DXA ($n = 8$/group). All animal experiments were approved by the Institutional Animal Care and Use Committee of The Affiliated Hospital of Jinggangshan University (2020-DL20).

Immunofluorescence (IF) assay

The OCPs (2×10^6) were seeded on 6-cm dishes and stimulated with the specified treatment. The treated OCPs were fixed with 4% paraformaldehyde (PFA). After perforation, the cells were blocked with 1% BSA and incubated with anti-TRAF3 antibody (sc-6933, 1:200; Santa Cruz Biotechnology, Texas, USA) at 4 °C overnight. Next, the cells were stained with fluorescent labelled secondary antibody for 30 min and then counterstained with DAPI for 10 min. Finally, the cells were observed under fluorescence microscope (Olympus IX71, Tokyo, Japan).

Haematoxylin-eosin (H&E), TRAP, and IF staining in bone tissues

The femurs of mice were fixed in 4% PFA for 40 h, decalcified with 10% EDTA (pH 7.3) at 4 °C for 2 weeks, then dehydrated with graded ethanol, and embedded in paraffin. The femoral sections (8 μm thick) were stained with H&E to observe the trabecular bone ($n = 8$/group); osteoclasts were evaluated by TRAP staining on corresponding sections ($n = 8$/group); and

TRAF3 fluorescence intensity in immature osteoclasts was identified by IF staining on corresponding sections (RANK, H-7, 1:200; TRAF3, 1:200; Santa Cruz Biotechnology) ($n = 6$/group). The trabecular area (%Tb.Ar) of the H&E-stained sections was analyzed using Image-Pro Plus (IPP) software. The osteoclast number of TRAP-stained sections was counted using an eyepiece grid. For IF assay, all sections were incubated in citrate buffer overnight at 60 °C to expose antigens. Subsequently, the sections were incubated overnight in the first antibody at 4 °C, and the secondary antibody was incubated for 1 hour at room temperature.

Statistical analysis

Statistical analyses were carried out using GraphPad Prism8 Software. The whole data are presented as the mean±SEM. For comparisons, one-way ANOVA and Student's t-test were performed as indicated. Tukey test was used for Post-hoc Multiple Comparisons. $p < 0.05$ was considered statistically significant.

RESULTS

LPS suppressed TRAF3 protein level in OCPs

Firstly, the effects of LPS on the expression patterns of TRAF3 in OCPs require the investigation. Western-blot experiments showed that LPS at the concentration from 20 to 100 ng/ml decreased the protein level of TRAF3 in a concentration-dependent manner in OCPs (Fig. 1a,b). Nevertheless, quantitative PCR results displayed that LPS did not affect the mRNA expression of TRAF3 except at 20 ng/ml (Fig. 1c). Immunofluorescence results also showed that LPS significantly inhibited the protein level of TRAF3 at 100 ng/ml (Fig. 1d). It was implied that LPS may promote the degradation of TRAF3 protein in OCPs.

LPS inhibited TRAF3 protein level of OCPs *in vivo*

Subsequently, we evaluated the *in vivo* role of LPS in the OCPs of the trabecular bone. DXA results showed that bone mass was significantly reduced with the addition of LPS (Fig. 2d). Likewise, H&E staining showed that the trabecular areas in LPS-treated mice obviously decreased (Fig. 2a,e). In addition, TRAP staining showed that the trabecular areas of LPS-treated mice had more osteoclasts (Fig. 2b,f). These data identified the effectiveness of LPS in our experimental system. Importantly, the double-immunofluorescence staining of RANK (a specific marker of OCPs) and TRAF3 on bone sections showed that compared with control mice, the TRAF3 level of the RANK$^+$ cells in trabecular bone of LPS-treated mice (defined as yellow overlapping fluorescence of TRAF3 and RANK) significantly declined (Fig. 2c). These data suggested that that LPS inhibits TRAF3 protein level in trabecular OCPs.
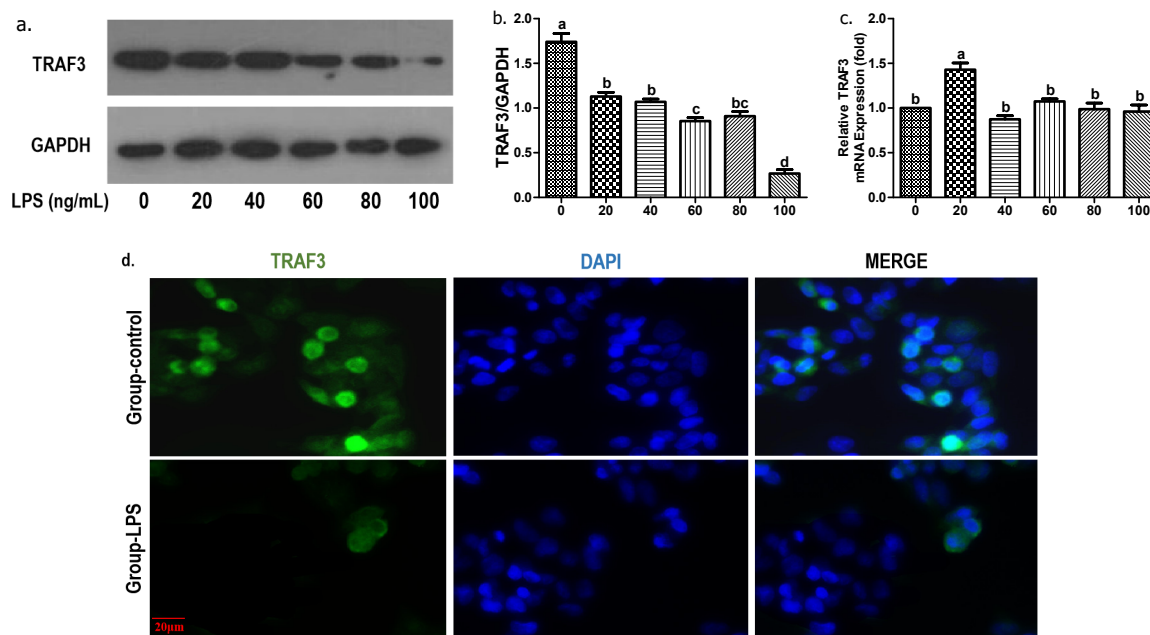
Fig. 1 LPS suppressed TRAF3 protein level in OCPs after 12 h treatment. (a,b) TRAF3 protein level in OCPs after treatment with different concentrations of LPS. (c) TRAF3 mRNA expression in OCPs after treatment with different concentrations of LPS. (a-c) Compared among each group, $p < 0.05$ by one-way ANOVA. The data are expressed as the mean ± SEM from 3 independent experiments. (d) TRAF3 fluorescent expression in OCPs after treatment with 100 ng/ml of LPS, yellow fluorescence indicates TRAF3 (scale bar, 20 μm). The data are representative images among 6 independent samples with consistent results.

LPS-induced osteoclastogenesis was repressed by TRAF3 overexpression

To further explore the relation between TRAF3 and LPS-regulated osteoclastogenesis, we observed the role of TRAF3 overexpression using gene transduction technology in the osteoclastogenesis treated by LPS. The results showed that TRAF3 overexpression reduced the number of LPS-induced osteoclasts (Fig. 3a-c), supporting that TRAF3 is involved in LPS-induced osteoclastogenesis. qPCR analyses related to osteoclastic genes showed the similar trends as the number of osteoclasts (MMP-9, TRAP, and CTSK) (Fig. 3d-f). As shown in Fig. 3g, TRAF3 overexpression partially recovered the reduced TRAF3 protein expression by LPS intervention, which demonstrated the effectiveness of our experimental system.

LPS-decreased TRAF3 protein level of OCPs was reversed by the application of chloroquine or bafilomycin

We documented that LPS inhibited TRAF3 protein level while no affecting TRAF3 mRNA expression in OCPs. Accordingly, we speculate that LPS could degrade TRAF3 protein in OCPs. As shown in Fig. 4a-c, LPS significantly increased LC3II protein expression and decreased p62 level in OCPs. However, treatment of chloroquine or bafilomycin increased LC3II and p62 protein level in OCPs both with and without LPS (Fig. 4a-c). Both chloroquine and bafilomycin could prevent the degradation of LC3 and p62 by blocking the fusion of autophagosome and lysosome. The above results supported the normal operation of autophagic flux. Thus, this experimental system based on autophagic inhibitors is reliable. As shown in Fig. 4a,d LPS significantly reduced TRAF3 level in OCPs, which was reversed by the addition of chloroquine or bafilomycin. These results indicated that LPS could degrade TRAF3 in OCPs through the activation of autophagy.

TRAF3 silencing partially reversed the inhibitory effect of chloroquine on LPS-induced osteoclastogenesis

Ultimately, we combined TRAF3 silencing with the application of autophagic inhibitors to further investigate the significance of autophagy-TRAF3 signaling in LPS-regulated osteoclastogenesis. The efficiency of TRAF3 silencing using RNA interference was determined in Fig. 5a. As shown in Fig. 5b,c the application of chloroquine significantly decreased the number of LPS-induced osteoclasts. Although TRAF3 silencing did not affect LPS-stimulated osteoclast differentiation level without chloroquine, it partially recovered the inhibition of LPS function by chloroquine (Fig. 5b,c). qPCR analyses regarding osteoclastic genes showed the similar trends as the number of osteoclasts (MMP-9, TRAP,
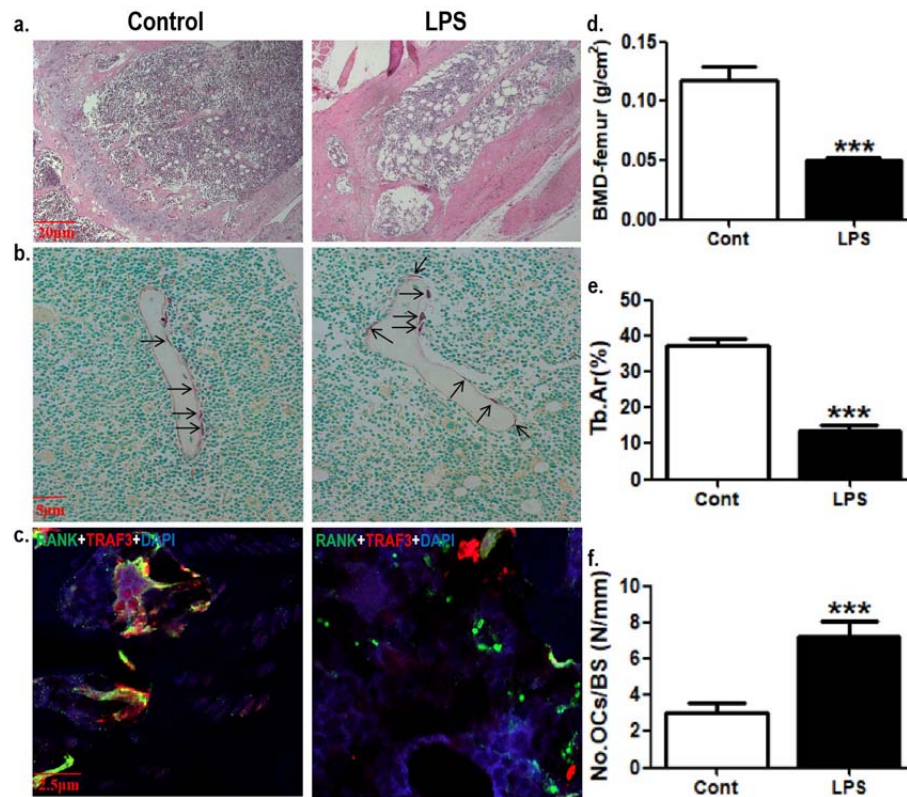
Fig. 2 LPS inhibited TRAF3 protein level of OCPs *in vivo*. (a) Representative H&E-stained femoral sections from corresponding mice (scale bar, 20 μm). (b) The typical TRAP-stained femoral sections (black arrowheads); scale bar, 5 μm. (c) Representative IF-stained femoral sections (green, RANK; red, TRAF3; and yellow, overlaps of RANK and TRAF3); scale bar, 2.5 μm. The data are representative images among 6 independent samples with consistent results. (d) Dual energy X-ray absorptiometry (DXA) analysis showing BMD at femurs ($n = 8$/group). (e) The trabecular area (%Tb.Ar) by H&E staining and IPP system ($n = 8$/group). (f) Osteoclast number per millimeter of trabecular surface ($n = 8$/group). The data are expressed as the mean ± SEM. *** $p < 0.001$ by Student's *t*-test. Cont, control group; LPS, LPS-treated group.
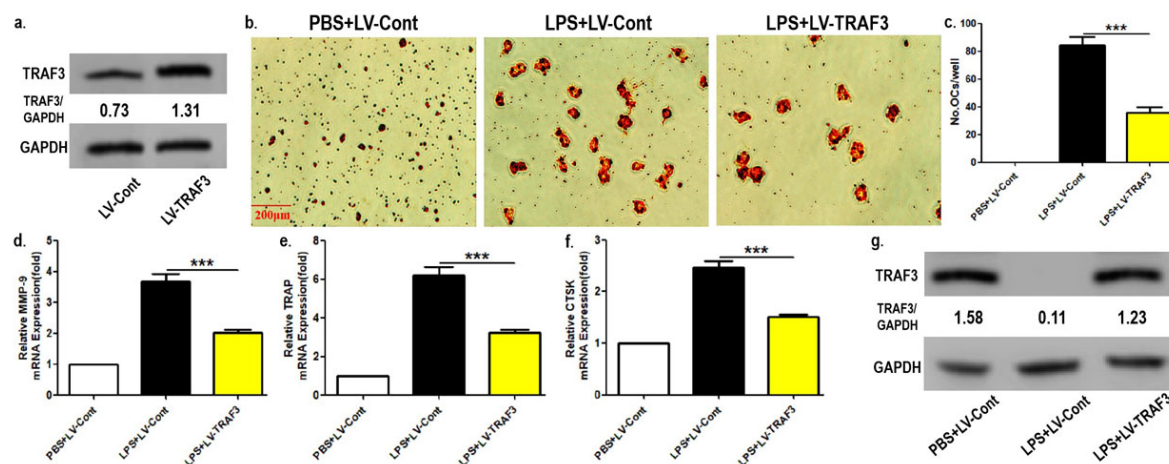

Fig. 3 LPS-induced osteoclastogenesis was repressed by TRAF3 overexpression. (a) TRAF3 protein level in corresponding OCPs. (b) Representative TRAP staining images of osteoclasts derived from corresponding OCPs (LPS: 100 ng/ml); scale bar, 200 μm. (c-f) The quantitative results regarding differentiated osteoclast number and the mRNA level of osteoclastic markers. (g) Protein level of TRAF3 in corresponding OCPs (intervention time: 12 h). The data are expressed as the mean ± SEM from 3 independent experiments: *** $p < 0.001$ by one-way ANOVA.
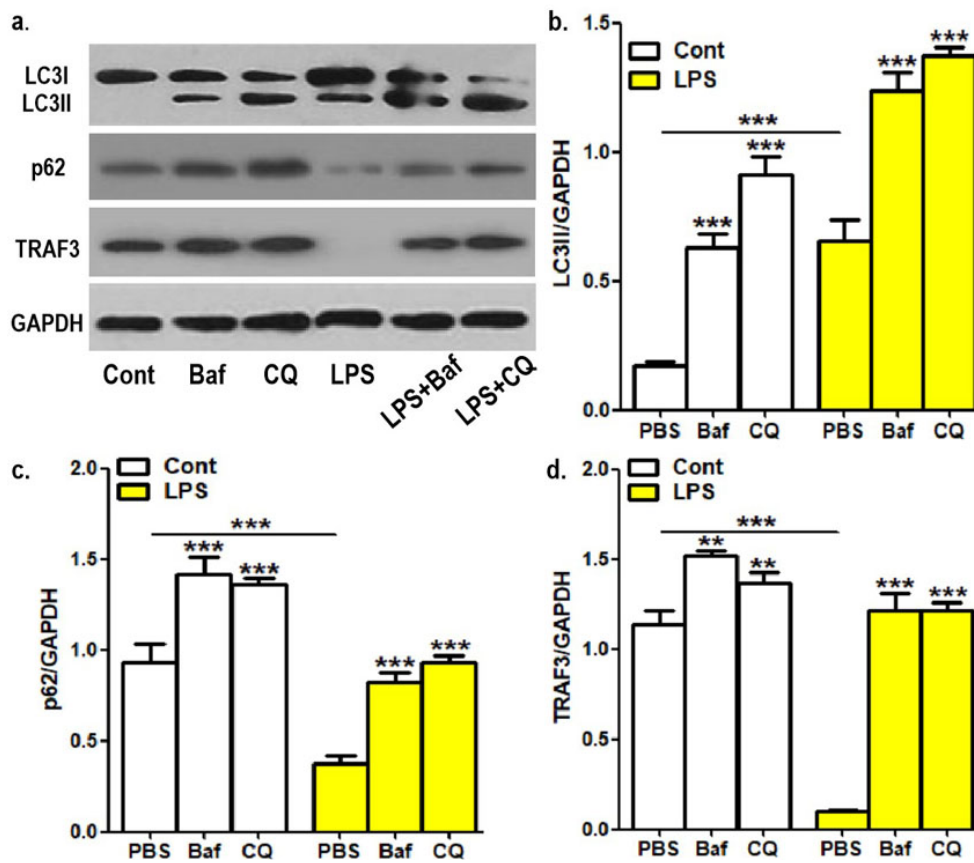
Fig. 4 LPS-decreased TRAF3 protein level of OCPs was reversed by chloroquine or bafilomycin. (a) The protein level of LC3, p62, or TRAF3 in corresponding OCPs (chloroquine: 10 μM; bafilomycin: 50 ng/ml; and intervention time: 12 h). (b-d) The quantitative results regarding the protein level of LC3II, p62, or TRAF3. The data are expressed as the mean ± SEM from 3 independent experiments: ** $p < 0.01$ and *** $p < 0.001$ by one-way ANOVA. Cont, control group; Baf, bafilomycin; and CQ, chloroquine.
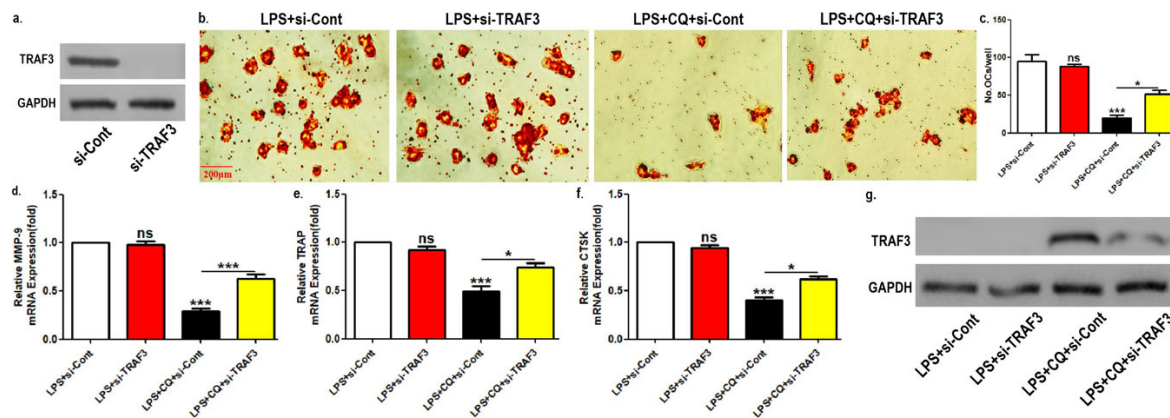

Fig. 5 TRAF3 silencing partially reversed the inhibition of chloroquine on LPS-induced osteoclastogenesis. (a) Protein level of TRAF3 in corresponding OCPs. (b) Representative TRAP staining images of osteoclasts derived from corresponding OCPs (scale bar, 200 μm). (c-f) The quantitative results regarding differentiated osteoclast number and the mRNA level of osteoclastic markers. (g) Protein level of TRAF3 in corresponding OCPs (intervention time: 12 h). The data are expressed as the mean ± SEM from 3 independent experiments: * $p < 0.05$ and *** $p < 0.001$ by one-way ANOVA. CQ, chloroquine.

and CTSK) (Fig. 5d-f). As shown in Fig. 5g, TRAF3 silencing did not affect TRAF3 protein expression in the presence of LPS, but TRAF3 silencing partially reversed the increased TRAF3 level by chloroquine, demonstrating the effectiveness of our experimental system.

DISCUSSION

In chronic infections caused by Gram-negative bacteria, the osteoclastic activity is enhanced, which results in osteolysis. However, the therapeutic methods of infection-related bone loss are limited. Thus, how to improve the treatment protocols of infection-related bone loss has become a challenge. LPS, a main component of the outer membrane of Gram-negative bacteria, is also a classical pro-osteoclastogenic factor [6–12]. Thus, exploring the potential mechanism regarding LPS-induced osteoclastogenesis is conducive to better solve the above challenge. LPS is considered an autophagic inducer, especially OCPs [28–31]. In view of the pivotal role of autophagy in degrading TRAF3, an important anti-osteoclastogenic factor [22–24], the intrinsic mechanism underlying LPS-regulated osteoclastogenesis can be better understood from autophagic perspective. The present study reveals the first evidence related to the role of LPS in enhancing the autophagic degradation of TRAF3, which results in the increased osteoclastogenesis.

Here, our experimental data *in vivo* and *in vitro* showed that LPS reduced TRAF3 protein level while keeping TRAF3 mRNA level stable in OCPs. It was suggested that LPS plays a role in TRAF3 degradation of OCPs. As a biological mechanism to maintain cell homeostasis, autophagy could decompose specific macromolecules. Therefore, we speculated that LPS could degrade TRAF3 proteins in OCPs through autophagic activation. The results displayed that LPS activated autophagy (shown in increased LC3II protein level and decreased p62 protein level) and decreased TRAF3 protein level. Furthermore, LPS-reduced TRAF3 proteins could be recovered by autophagic inhibition with chloroquine or bafilomycin. Consistent with our conjecture, these results confirmed the role of autophagy in LPS-regulated TRAF3 degradation in OCPs. In addition, TRAF3 overexpression could reverse the induction of LPS on the osteoclastogenesis, demonstrating that TRAF3 participates in LPS-regulated osteoclastogenesis. More importantly, chloroquine inhibited LPS-induced osteoclastogenesis, which was partially reversed by TRAF3 knockdown. The role of autophagy-TRAF3 signaling in LPS-regulated osteoclastogenesis was also confirmed. Taken together, LPS could activate autophagy, subsequently degrade TRAF3 in OCPs, and ultimately promote the osteoclastogenesis. Therefore, for infection-related bone loss, any method that helps to increase TRAF3 expression or inhibit autophagic degradation
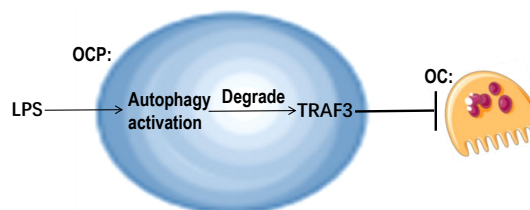

Fig. 6 The schematic diagram regarding autophagy-TRAF3 signaling in OCPs regulated by LPS during LPS-induced osteoclastogenesis.

of TRAF3 in OCPs may be an effective adjuvant therapy. The corresponding working model is described in Fig. 6. In addition, it should be noted that TRAF3 silencing had no effect on LPS function in the absence of chloroquine. Previous studies showed that in RANKL-induced osteoclastogenesis, RANKL promoted the degradation of TRAF3, resulting in the fact that the application of RNAi has no effect on the downregulation of TRAF3 level [23, 32]. Like RANKL function, RNAi application also did not affect the further changes of TRAF3 following LPS-degraded TRAF3 molecules of OCPs (Fig. 5g), which can explain the invalidity of TRAF3 silencing when lacking autophagic inhibition.

CONCLUSION

From the perspective of autophagic response, our study provided for the first time a novel mechanism underlying LPS-induced osteoclastogenesis. Our data clarified the role of LPS in promoting TRAF3 degradation due to its promotion on autophagic activity, which participates in LPS-regulated osteoclastogenesis. Our study shed lights on improving the treatment strategies of infection-related bone loss.

REFERENCES

1. Zhao C, Irie N, Takada Y, Shimoda K, Miyamoto T, Nishiwaki T, Suda T, Matsuo K (2006) Bidirectional ephrinB2-EphB4 signaling controls bone homeostasis. *Cell Metab* **4**,111–121.
2. Nair SP, Meghji S, Wilson M, Reddi K, White P, Henderson B (1996) Bacterially induced bone destruction: mechanisms and misconceptions. *Infect Immun* **64**, 2371–2380.
3. Keestra JA, Grosjean I, Coucke W, Quirynen M, Teughels W (2014) Non-surgical periodontal therapy with systemic antibiotics in patients with untreated aggressive periodontitis: a systematic review and meta-analysis. *J Periodontal Res* **50**, 689–706.
4. Bohannon JK, Hernandez A, Enkhbaatar P, Adams WL, Sherwood ER (2013) The immunobiology of toll-like receptor 4 agonists: from endotoxin tolerance to immunoadjuvants. *Shock* **40**, 451–462.

5. Lee YM, Kim IS, Lim BO (2021) Effect of sandalwood oil on inhibition of reactive oxygen species generation and lipopolysaccharide-induced inflammation through down-regulation of the nuclear factor-κB signaling pathways. *ScienceAsia* **47**, 277–286.

6. Suda K, Udagawa N, Sato N, Takami M, Itoh K, Woo JT, Takahashi N, Nagai K (2004) Suppression of osteoprotegerin expression by prostaglandin E2 is crucially involved in lipopolysaccharide-induced osteoclast formation. *J Immunol* **172**, 2504–2510.

7. Islam S, Hassan F, Tumurkhuu G, Dagvadorj J, Koide N, Naiki Y, Mori I, Yoshida T, et al (2007) Bacterial lipopolysaccharide induces osteoclast formation in RAW264.7 macrophage cells. *Biochem Biophys Res Commun* **360**, 346–351.

8. Hotokezaka H, Sakai E, Ohara N, Hotokezaka Y, Gonzales C, Matsuo K, Fujimura Y, Yoshida N, et al (2006) Molecular analysis of RANKL-independent cell fusion of osteoclast-like cells induced by TNF-α, lipopolysaccharide, or peptidoglycan. *J Cell Biochem* **101**, 122–134.

9. He L, Duan H, Li X, Wang S, Zhang Y, Lei L, Xu J, Liu S, et al (2016) Sinomenine down-regulates TLR4/TRAF6 expression and attenuates lipopolysaccharide-induced osteoclastogenesis and osteolysis. *Eur J Pharmacol* **779**, 66–79.

10. Khuda II, Koide N, Noman AS, Dagvadorj J, Tumurkhuu G, Naiki Y, Komatsu T, Yoshida T, et al (2010) Seladin-1 is a novel lipopolysaccharide (LPS)-responsive gene and inhibits the tumour necrosis factor-α production and osteoclast formation in response to LPS. *Immunology* **131**, 59–66.

11. Guo C, Hou GQ, Li XD, Xia X, Liu DX, Huang DY, Du SX (2012) Quercetin triggers apoptosis of lipopolysaccharide (LPS)-induced osteoclasts and inhibits bone resorption in RAW264.7 cells. *Cell Physiol Biochem* **30**, 123–136.

12. Hou GQ, Guo C, Song GH, Fang N, Fan WJ, Chen XD, Yuan L, Wang ZQ (2013) Lipopolysaccharide (LPS) promotes osteoclast differentiation and activation by enhancing the MAPK pathway and COX-2 expression in RAW264.7 cells. *Int J Mol Med* **32**, 503–510.

13. Ke D, Ji L, Wang Y, Fu X, Chen J, Wang F, Zhao D, Xue Y, et al (2019) JNK1 regulates RANKL-induced osteoclastogenesis via activation of a novel Bcl-2-Beclin1-autophagy pathway. *FASEB J* **33**, 11082–11095.

14. Ke D, Wang Y, Yu Y, Wang Y, Zheng W, Fu X, Han J, Zhang G, et al (2020) Curcumin-activated autophagy plays a negative role in its anti-osteoclastogenic effect. *Mol Cell Endocrinol* **500**, ID 110637.

15. Cheng L, Zhu Y, Ke D, Xie D (2020) Oestrogen-activated autophagy has a negative effect on the anti-osteoclastogenic function of oestrogen. *Cell Prolif* **53**, e12789.

16. Zheng Z, Zhang X, Huang B, Liu J, Wei X, Shan Z, Wu H, Feng Z, et al (2021) Site-1 protease controls osteoclastogenesis by mediating LC3 transcription. *Cell Death Differ* **28**, 2001–2018.

17. Park HJ, Gholam-Zadeh M, Suh JH, Choi HS (2019) Lycorine attenuates autophagy in osteoclasts via an axis of mROS/TRPML1/TFEB to reduce LPS-induced bone loss. *Oxid Med Cell Longev* **2019**, 8982147.

18. Laha D, Deb M, Das H (2019) KLF2 (kruppel-like factor 2 [lung]) regulates osteoclastogenesis by modulating autophagy. *Autophagy* **15**, 2063–2075.

19. Häcker H, Tseng PH, Karin M (2011) Expanding TRAF function: TRAF3 as a tri-faced immune regulator, *Nat Rev Immunol* **11**, 457–468.

20. Devergne O, Hatzivassiliou E, Izumi KM, Kaye KM, Kleijnen MF, Kieff E, Mosialos G (1996) Association of TRAF1, TRAF2, and TRAF3 with an Epstein-Barr virus LMP1 domain important for B-lymphocyte transformation: role in NF-kappaB activation. *Mol Cell Biol* **16**, 7098–7108.

21. Rothe M, Sarma V, Dixit VM, Goeddel DV (1995) TRAF2-mediated activation of NF-kappa B by TNF receptor 2 and CD40. *Science* **269**, 1424–1427.

22. Xiu Y, Xu H, Zhao C, Li J, Morita Y, Yao Z, Xing L, Boyce BF (2014) Chloroquine reduces osteoclastogenesis in murine osteoporosis by preventing TRAF3 degradation. *J Clin Invest* **124**, 297–310.

23. Ke D, Zhu Y, Zheng W, Fu X, Chen J, Han J (2019) Autophagy mediated by JNK1 resists apoptosis through TRAF3 degradation in osteoclastogenesis. *Biochimie* **167**, 217–227.

24. Xue Y, Liang Z, Fu X, Wang T, Xie Q, Ke D (2019) IL-17A modulates osteoclast precursors' apoptosis through autophagy-TRAF3 signaling during osteoclastogenesis. *Biochem Biophys Res Commun* **508**, 1088–1092.

25. Chen M, Liu J, Yang W, Ling W (2017) Lipopolysaccharide mediates hepatic stellate cell activation by regulating autophagy and retinoic acid signaling. *Autophagy* **13**, 1813–1827.

26. Lei S, Liu XM, Liu Y, Bi J, Zhu S, Chen X (2020) Lipopolysaccharide downregulates the osteo-/odontogenic differentiation of stem cells from apical papilla by inducing autophagy. *J Endod* **46**, 502–508.

27. Wang XH, Zhang ZH, Cai XL, Ye P, Feng X, Liu TT, Li XZ (2017) Lipopolysaccharide induces autophagy by targeting the AMPK-mTOR pathway in human nasal epithelial cells. *Biomed Pharmacother* **96**, 899–904.

28. Sul OJ, Park HJ, Son HJ, Choi HS (2017) Lipopolysaccharide (LPS)-induced autophagy is responsible for enhanced osteoclastogenesis. *Mol Cells* **40**, 880–887.

29. Park HJ, Son HJ, Sul OJ, Suh JH, Choi HS (2018) 4-Phenylbutyric acid protects against lipopolysaccharide-induced bone loss by modulating autophagy in osteoclasts. *Biochem Pharmacol* **151**, 9–17.

30. Sul OJ, Sung YB, Rajasekaran M, Ke K, Yu R, Back SH, Choi HS (2018) MicroRNA-155 induces autophagy in osteoclasts by targeting transforming growth factor β-activated kinase 1-binding protein 2 upon lipopolysaccharide stimulation. *Bone* **116**, 279–289.

31. Chen L, Yang Y, Bao J, Wang Z, Xia M, Dai A, Tan J, Zhou L, et al (2020) Autophagy negative-regulating Wnt signaling enhanced inflammatory osteoclastogenesis from Pre-OCs *in vitro*. *Biomed Pharmacother* **126**, 110093.

32. Yao Z, Xing L, Boyce BF (2009) NF-kappaB p100 limits TNF-induced bone resorption in mice by a TRAF3-dependent mechanism. *J Clin Invest* **119**, 3024–3034.